CrystEngComm

Cite this: *CrystEngComm*, 2012, **14**, 4589–4595

www.rsc.org/crystengcomm

PAPER

Anion-dependent coordinative networking of macrocycle with copper(I) halides†

In-Hyeok Park,‡ Hyun Jee Kim‡ and Shim Sung Lee*

Received 24th January 2012, Accepted 19th April 2012
DOI: 10.1039/c2ce25111f

An O_2S_2-macrocycle **L** incorporating three aromatic subunits was synthesized and structurally characterized by X-ray analysis. Four coordination polymers of **L** with copper(I) halides (Cl, Br and I) adopting different topologies and network patterns depending on the anions are reported. Reactions of **L** with copper(I) chloride and copper(I) bromide yielded a single-stranded one-dimensional (1D) coordination polymer $[CuCl_2(\mathbf{L})(CH_3CN)]_n$ (**1**) with an oxidized copper(II) centre and a double-stranded 1D coordination polymer $[(Cu_2Br_2)(\mathbf{L})_2]\cdot 4CH_2Cl_2]_n$ (**2**), with each strand linked by a rhomboid-type Cu_2Br_2 unit. However, the reaction with copper(I) iodide under the same conditions gave an emissive mixture of supramolecular isomers with an identical composition $\{[Cu_4I_4(\mathbf{L})_2]\cdot CH_2Cl_2\}_n$, adopting a regular (**3a**) and a tilted (**3b**) square-grid-type 2D coordination polymers *via* cubane-type Cu_4I_4 linking. The XRPD results also confirmed the binary mixture. The conformational diversity in the ligand leads to a variation in overall structural motifs of the supramolecular isomers.

Introduction

The sulfur-containing macrocycles, called thiacrowns or thiamacrocycles, often form not only discrete type endocyclic metallo-supramolecules but also infinite *exo*-coordination-based networks in which some soft metal ions exist inside or outside the macrocyclic cavity, respectively.[1] In particular, the exocyclic soft metal coordination networks with bridging coordinative anions have been our interest because of their attractive high dimensional structures and physical properties.[2] Several cases of the *exo*-coordination-based mono- and multinuclear complexes of thiamacrocycles with an infinite form have been introduced by us[2] and others.[3] We have also suggested that such *endo*- and *exo*-coordination can be controlled by the choice of the anions with different coordination abilities.[4] Based on this behaviour, we have proposed an *N*-azo-coupled NS_2O_2-macrocycle system, which illustrates how the coordinating ability of the anion controls a colour change through formation of *endo*- or *exo*-metal complexes.[5] Very recently, we also reported the 1D and 2D network coordination products of tribenzo-O_2S_2-macrocycle isomers incorporating a xylyl group in the *ortho*-, *meta*- and *para*- (**L** in this work) positions with mercury(II) thiocyanate.[6] In this case, all the polymeric products show different topologies not only because of the variation of ligand rigidity but also diverse bridging modes of the thiocyanate ion.

Among the soft metal salts employed in the above system, copper(I) halides are particularly interesting because of their $(CuX)_n$-type cluster-based networking *via* its thiaphilic nature associated with photoluminescence properties.[7] The copper(I) halides as a versatile member in coordination chemistry and crystal engineering for noncyclic multidentate ligands are well documented and reviewed.[8] In this case, however, a prediction of the resulting structure still remains challenging. Furthermore, no systematic structural work for the thiamacrocycles has been reported so far for copper(I) coordination polymers with different halide anions.[9] So we have focused our attention on the halide anions which could potentially influence the resulting products because of their different size, reactivity and so on.[8,10]

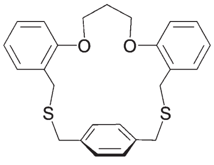

L

In connection with these reasons, we were motivated to employ a tribenzo-O_2S_2-macrocycle **L** in which the two sulfur donors are linked with the *para*-xylyl unit, giving inherent macrocyclic ring rigidity and inducing the *exo*-coordination of sulfur donors. A combination of the anion variation of the copper(I) halides and the tendency for the *exo*-coordination of **L** can serve as versatile controlling factors for the assembly of the

---

Department of Chemistry and Research Institute of Natural Science, Gyeongsang National University, Jinju, 660-701, S. Korea. E-mail: sslee@gnu.ac.kr

† Electronic supplementary information (ESI) available: XRPD patterns of **1** and **2**, TGA of **1**, **2** and **3**, NMR spectra of **L**, EPR spectrum of **1**. CCDC reference numbers 863927–863931. For ESI and crystallographic data in CIF or other electronic format see DOI: 10.1039/c2ce25111f/

‡ These two authors contributed equally to this work.

final structures of the respective polymeric networks, adopting 1D and 2D features as depicted in Scheme 1. In particular, we report the structural characteristics of two supramolecular isomers of the copper(I) iodide coordination polymer, one of which is a regular square-grid type isomer while the other adopts a tilted square-grid analogue.

Results and discussion

Synthesis of ligand

Synthesis of **L** began with salicylaldehyde (Scheme 2). The dichloride precursor for the cyclisation was prepared through the dialdehyde and dialcohol.[11] **L** was obtained by coupling reaction between the dichloride precursor and 1,4-benzenedimethanethiol in the presence of Cs_2CO_3 under high dilution condition in a reasonable yield (65%).

L was also characterized in the solid state by single-crystal X-ray crystallography. Colourless single crystals of **L** suitable for X-ray analysis were obtained by slow evaporation of its dichloromethane solution. The crystal structure is shown in Fig. 1. As expected, the two sulfur donors are oriented in an exodentate fashion while the two oxygen atoms are arranged endodentate with respect to the ring cavity which adopts a nearly flat arrangement. The S···S distance in the macrocycle is 7.166 Å. The aliphatic ring segment corresponding to O1–C–C–C–O2 shows a *gauche–anti* arrangement in keeping with the more flexible nature than the restricted S2–C-Ar–C–S1 segment.

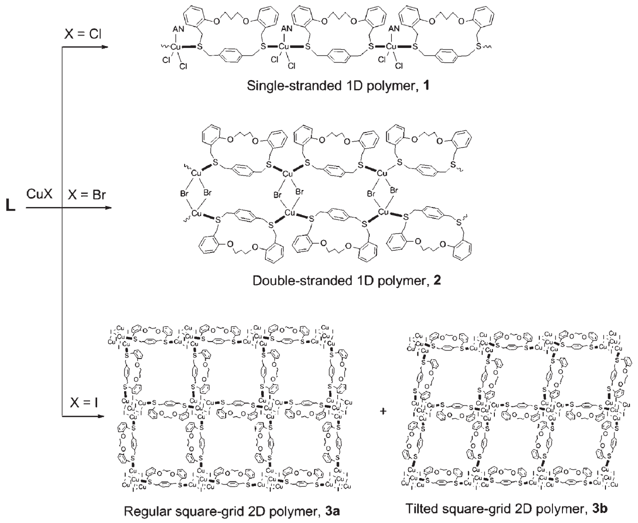

Scheme 1 Structural diversity of copper halides complexes of **L**.

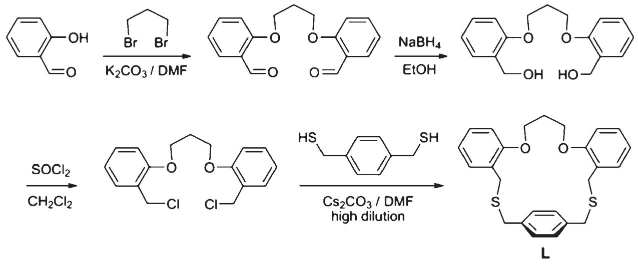

Scheme 2 Synthesis of **L**.

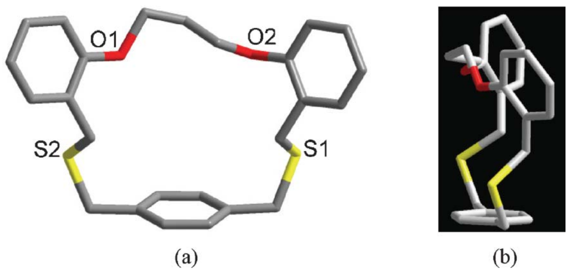

(a) (b)

Fig. 1 Crystal structure of **L**: (a) front view and (b) side view.

Preparation and structural description of 1D copper chloride and bromide complexes (1 and 2)

The reaction of **L** with copper(I) chloride in an acetonitrile–dichloromethane mixture resulted in an initial colourless reaction mixture changing to green within 30 min at room temperature. Slow evaporation of the green solution afforded a high yield of a brown crystalline product **1** suitable for X-ray analysis. The reaction solution and crystal colour together with its elemental analysis initially suggested that it was a Cu(II) species and subsequently confirmed by a crystal structure determination (Fig. 2) and its EPR spectrum (Fig. S7†); selected geometric parameters are presented in Table 1. The X-ray analysis reveals that **1** features a 1D polymeric array of formula $[Cu(\mathbf{L})Cl_2(CH_3CN)]_n$ with an *exo*-coordination mode. The homogeneity of the product was confirmed by the XRPD patterns (Fig. S1†). The framework shows a –**L**–Cu–**L**–Cu– pattern and its asymmetric unit contains one **L**, one Cu atom, two Cl atoms and one acetonitrile. The copper atom that lies outside the cavity is five-coordinated and is bonded to two S atoms from two adjacent **L**, two chloride ions and one acetonitrile. The coordination geometry around the copper atom can be described as a distorted trigonal bipyramid where Cl1, Cl2 and N1 form the trigonal plane while S1 and S2A atoms occupy the axial positions [∠S1–Cu1–S2A 169.66(2)°].

Slow diffusion of a dichloromethane solution of **L** into an acetonitrile solution of copper(I) bromide afforded a pale yellow crystalline complex **2**. The complex **2** is a double-stranded 1D polymer of formula $\{[(Cu_2Br_2)(\mathbf{L})_2]\cdot 4CH_2Cl_2\}_n$ (Fig. 3); selected geometric parameters are presented in Table 2. The homogeneity of the product was confirmed by the XRPD patterns (Fig. S2†). The successive ligand molecules are linked with Cu-(μ_2-Br)$_2$-Cu rhomboid units *via* Cu–S bonds. The Cu(I) coordination sphere is distorted tetrahedral, with the Cu-donor atom angles falling in the range 103.09(2)–122.85(2)°. In **2**, the intra- and interligand S···S distances are 7.758 and 4.005 Å, respectively. The Cu–S bond distances [2.269(1) and 2.292(1) Å] agree well with the corresponding values [2.226–2.899 Å] for related systems.[12] Not surprisingly given their hard nature, neither of the oxygen donors of **L** participates in coordination. With respect to this

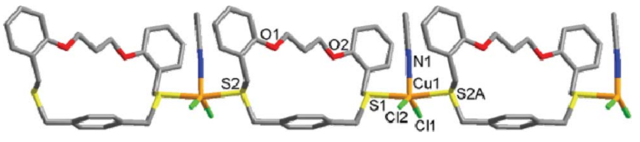

Fig. 2 Single-stranded 1D polymeric structure of **1**, $[Cu(\mathbf{L})Cl_2(CH_3CN)]_n$.

Table 1 Selected bond lengths [Å] and bond angles [°] for **1**[a]

Cu1–S1	2.355(1)	Cu1–S2A	2.363(1)
Cu1–N1	2.191(2)	Cu1–Cl1	2.266(1)
Cu1–Cl2	2.260(1)		
S1–Cu1–S2A	169.66(2)	N1–Cu1–S1	84.29(4)
N1–Cu1–S2A	85.37(4)	N1–Cu1–Cl1	111.73(5)
N1–Cu1–Cl2	111.73(5)	Cl1–Cu1–Cl2	136.62(2)
Cl2–Cu1–S1	88.355(19)	Cl1–Cu1–S1	96.678(18)
Cl2–Cu1–S2A	95.633(19)	Cl1–Cu1–S2A	86.985(18)

[a] Symmetry codes: (A) $x - 1, y, z$.

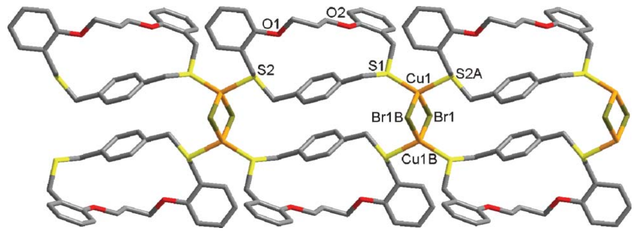

Fig. 3 Double-stranded 1D polymeric structure of **2**, $\{[(Cu_2Br_2)(\mathbf{L})_2]\cdot 4CH_2Cl_2\}_n$. The non-coordinating solvent molecules are omitted.

Table 2 Selected bond lengths [Å] and bond angles [°] for **2**[a]

Cu1–S1	2.269(1)	Cu1–S2A	2.292(1)
Cu1–Br1	2.542(1)	Cu1–Br1B	2.472(1)
Cu1–Cu1B	2.927(1)		
S1–Cu1–S2A	122.85(2)	S1–Cu1–Br1B	111.43(2)
S2A–Cu1–Br1B	105.94(2)	S1–Cu1–Br1	103.99(2)
Br1–Cu1–S2A	103.094(19)	Br1–Cu1–Br1B	108.577(13)

[a] Symmetry codes: (A) $x, y + 1, z$; (B) $-x, -y + 1, -z + 1$.

pattern, similar copper(I) halide complexes of two O_2S_2-macrocycles have been previously reported by us.[13]

Preparation and structural description of 2D copper iodide complexes (3a and 3b)

Slow diffusion of a dichloromethane solution of **L** into an acetonitrile solution of copper(I) iodide yielded a pale yellow crystalline product. X-ray analysis confirmed a mixture of two supramolecular isomers with an identical chemical composition of $\{[Cu_4I_4(\mathbf{L})_2]\cdot CH_2Cl_2\}_n$; a regular square-grid type 2D coordination polymer (**3a**) and a tilted square-grid analogue (**3b**) (Fig. 4 and Fig. S8†). Selected geometric parameters are presented in Tables 3 and 4. The comparison of the XRPD results for the synthesized product with the simulated data for **3a** and **3b** also confirmed that the product prepared is the binary mixture (Fig. 5). Separation of the mixed products was not possible but the expected content of **3b** in the mixture is less than 5% as a minor product. To figure out the more stable phase in the mixed phases (**3a** and **3b**), the XRD patterns at different periods (fresh product and after eight months) were compared, but no significant differences were observed.

The crystal structures of **3a** and **3b** are similar except that **3a** has a rectangular unit whereas **3b** possesses a rhomboidal one due to its inclined structure. In fact, one side of the square-grid network in **3b** is tilted to 14°. In both cases, the asymmetric unit contains two **L** molecules, one Cu_4I_4 cubane core and one CH_2Cl_2 solvent molecule (Fig. 4a). Interestingly, the Cu_4I_4 core whose geometry resembles a distorted cube with alternating vertices of Cu and I atoms is coordinated by four different ligands *via* Cu–S bonds (Fig. 4b). In two isomers, the Cu_4I_4 cores show no major differences in their geometric parameters. Also the Cu–S bond distances in both cases are quite similar. Each Cu atom is tetrahedrally coordinated to three μ_3-I atoms and one S donor of **L**, with the 'tetrahedral' angles falling in the range 99.99(3)–114.03(3)° for **3a** and 94.71(4)–119.85(4)° for **3b**. The larger dislocation from the regular tetrahedral angle for **3b** corresponds to its tilted conformation. Each **L** acts as a *bis*-monodentate ligand and connects the two Cu_4I_4 cores to form a $[(Cu_4I_4)_4(\mathbf{L})_4]$ unit with sides of 14.0 × 14.2 Å in **3a** and 13.5 × 14.3 Å in **3b** and diagonal distances of 18.2 × 21.6 Å in **3a** and 17.1 × 21.8 Å in **3b** (Fig. 4c). The square-grid networks are not planar but undulating due to the tetrahedral geometry of the Cu atoms. Because of the compact layer-to-layer packing of the undulating square-grid sheet, the intersections of the grid in **3a** and **3b** give almost no cavities (Fig. S8†). In both cases, one dichloromethane molecule exists inside each unit.

To understand the conformational difference of the two isomers, it is necessary to compare the conformation of **L** in **3a** and **3b**. As already mentioned above, the *para*-xylyl unit in **L** has an intrinsic rigidity but the dibenzo-ether unit is more flexible because of the $–O(CH_2)_3O–$ segment. Therefore, the conformation of **L** in each isomer is responsible for the torsion angles between atoms in the $–O(CH_2)_3O–$ segment. Both of the two independent **L** molecules in **3a** exhibit the *gauche–anti* conformation which means that the two ligands are similarly somewhat twisted upon complexation. While the two independent **L** molecules in **3b** show different conformations, adopting *gauche–anti* and *anti–anti*; the former is twisted and latter is quite flat. All these data indicate the relative conformation of **L** which is responsible for the discriminated square-grids **3a** and **3b**. In other words, the conformational diversity in ligand **L** leads to a variation in overall structural motifs.

Solid-state photoluminescence studies were carried out at room temperature (Fig. 6). Complexes **1** and **2** incorporating the trigonal bipyramidal Cu(II) geometry and the rhomboidal Cu_2Br_2 core, respectively, were found to be non-emissive. In contrast, the compound **3a** (with small amount of **3b**), adopting square-grid incorporating Cu_4I_4 cubane unit exhibits a broad band with a bright green emission maximum at 537 nm, the latter reflecting a cluster-centred (CC) excited state with mixed halide-to-metal charge transfer character (X/MLCT).[14] In other words, the photoluminescence of $Cu_4X_4(\mathbf{L})_4$ unit in **3a** and **3b** can come from either the charge transfer from the halide-Cu metals to the ligands (X/MLCT) or can arise from the d manifolds to an empty p orbital of the Cu_4 centre (CC).[7,14] Similar emission bands (530–550 nm) originated from the Cu_4I_4 cubane-type cluster have been also reported previously by us[2e,15] and the D. Li group.[8]

As a comparative study, it is noteworthy that both the copper(I) bromide and copper(I) iodide lead to the formation of the anion-assisted networking, but they show different dimensionalities and nuclearity. In formation of **3** (iodide), the cubane-type Cu_4I_4 core with higher nuclearity probably induces the higher dimensionality. In other words, the preferred 2D structure of **3** with higher dimensionality and nuclearity could be explained by the iodide ion being more reactive as a softer base than the bromide ion which gives the 1D structure in **2**. The

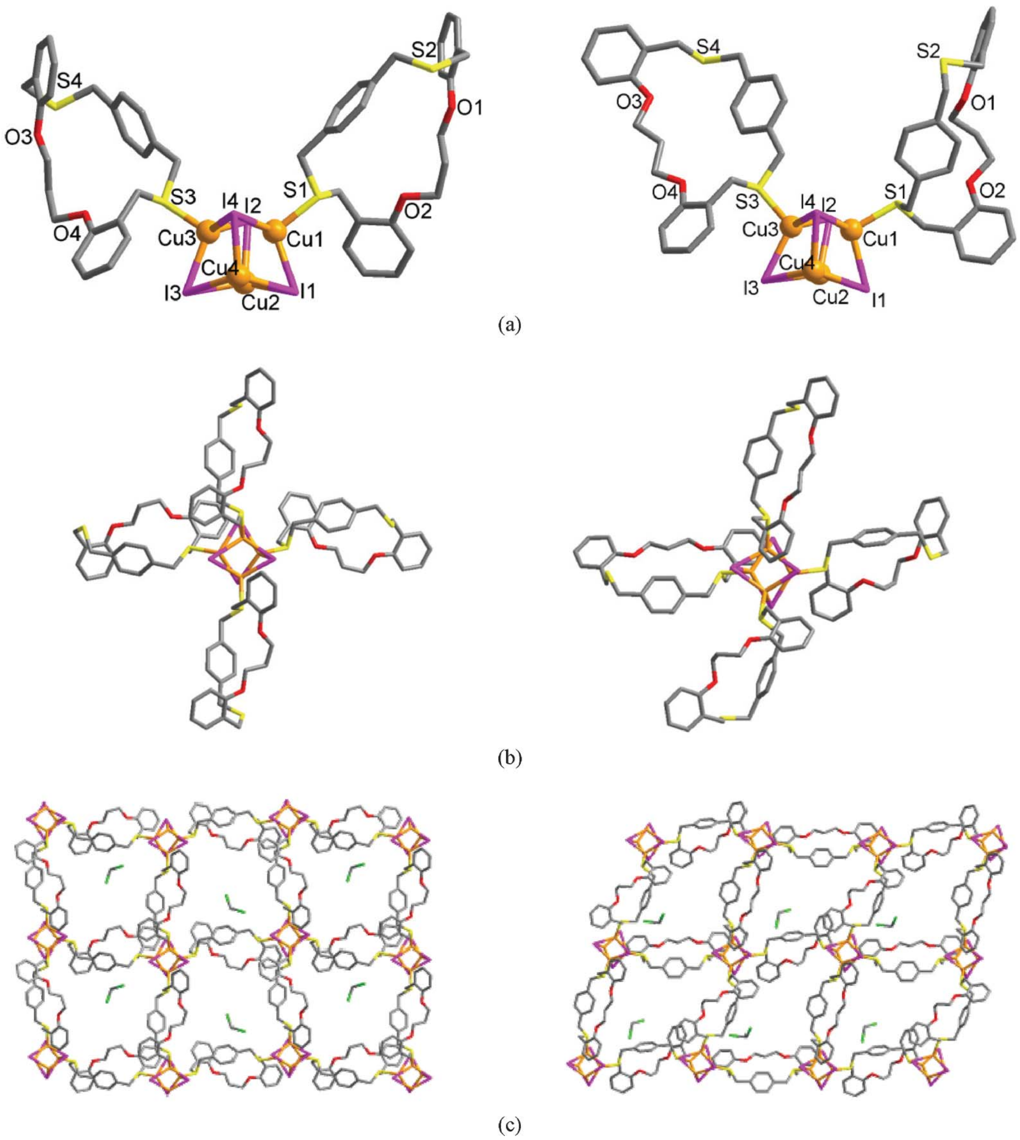

Fig. 4 Comparison of the 2D network structures of (*left*) **3a**, $\{[Cu_4I_4(\mathbf{L})_2]\cdot CH_2Cl_2\}_n$ and (*right*) **3b**, $\{[Cu_4I_4(\mathbf{L})_2]\cdot CH_2Cl_2\}_n$: (a) asymmetric units, (b) basic coordination environments, (c) square-grid structures.

observed oxidation of copper(I) to copper(II) in the chloride system for **1** can be considered because of the instability of CuCl in solution and also can be, in part, explained due to the lower reactivity of chloride ions compared to bromide and iodide ions towards the copper(I) centre.

Conclusions

Altering the copper(I) halide from chloride to iodide in complexation with the thiaoxamacrocycle **L** causes a shift from a 1D to a 2D anion-bridged framework. Copper(I) chloride under the same reaction conditions results in a 1D framework with an oxidized copper(II) centre and terminal chloride coordination in terminal positions. In particular, the 2D product derived from copper(I) iodide was revealed as an emissive mixture of supramolecular isomers, adopting regular and tilted square grids *via* cubane-type Cu_4I_4 linking. In this case, the conformational diversity in the ligand leads to a variation in the overall structural motifs of the supramolecular isomers. Consequently, the driving forces of the complexations are mainly based on the higher reactivity between soft acids [copper(I)] and soft bases [sulfur and halides]. Since the order of softness for the halides is $I^- > Br^- > Cl^-$, the softer anions gave the more complex products with larger sizes or higher dimensionalities.

Experimental section

General procedures

All chemicals and solvents used in the syntheses were of reagent grade and were used without further purification. NMR spectra were recorded on a Bruker 300 spectrometer (300 MHz). The FT-IR spectra were measured with a Thermo Fisher Scientific Nicolet *i*S 10 FT-IR spectrometer. The electrospray ionization (ESI) mass spectra were obtained on a Thermo Scientific LCQ Fleet spectrometer. The elemental analysis of **L**, **1**, **2** and **3** were

Table 3 Selected bond lengths [Å] and bond angles [°] for **3a**[a]

Cu1–Cu2	2.727(1)	Cu1–Cu3	2.719(1)
Cu1–Cu4	2.744(1)	Cu2–Cu4	2.691(1)
Cu2–Cu3	2.707(1)	Cu3–Cu4	2.780(1)
Cu1–I1	2.658(1)	Cu1–I4	2.713(1)
Cu1–I2	2.667(1)	Cu1–S1A	2.298(1)
Cu2–I1	2.615(1)	Cu2–I2	2.774(1)
Cu2–I3	2.666(1)	Cu2–S2	2.296(1)
Cu3–I4	2.656(1)	Cu3–I2	2.683(1)
Cu3–I3	2.667(1)	Cu3–S3	2.282(1)
Cu4–I1	2.667(1)	Cu4–I4	2.620(1)
Cu4–I3	2.707(1)	Cu4–S4B	2.319(1)
I1–Cu1–I2	112.31(2)	I1–Cu1–I4	111.16(2)
I2–Cu1–I4	112.28(2)	I1–Cu1–S1A	109.26(3)
I2–Cu2–S2	102.90(3)	I3–Cu2–S2	102.37(3)
I2–Cu2–I3	111.86(2)	I1–Cu2–S2	113.25(3)
I1–Cu2–I2	110.28(2)	I1–Cu2–I3	115.30(2)
I4–Cu1–S1A	102.81(3)	I2–Cu1–S1A	108.53(3)
I2–Cu3–I4	113.60(2)	I3–Cu3–I4	109.14(2)
I2–Cu3–S3	99.99(3)	I2–Cu3–I3	114.80(2)
I4–Cu3–S3	114.03(3)	I3–Cu3–S3	104.79(3)
I1–Cu4–I4	113.886(19)	I1–Cu4–I3	112.224(19)
I3–Cu4–I4	109.03(2)	I1–Cu4–S4B	102.67(4)
I3–Cu4–S4B	103.19(3)		

[a] Symmetry codes: (A) $x, y - 1, z$; (B) $x, -y + 1, z + 1/2$.

Table 4 Selected bond lengths [Å] and bond angles [°] for **3b**[a]

Cu1–Cu2	2.770(9)	Cu1–Cu3	2.654(1)
Cu1–Cu4	2.755(10)	Cu2–Cu3	2.675(1)
Cu3–Cu4	2.662(9)	Cu2–Cu4	2.747(1)
Cu1–I1	2.690(8)	Cu1–I2	2.652(1)
Cu1–I4	2.697(8)	Cu1–S1	2.321(2)
Cu2–I1	2.687(8)	Cu2–I2	2.658(1)
Cu2–I3	2.679(8)	Cu2–S4A	2.295(2)
Cu3–I2	2.765(8)	Cu3–I3	2.645(1)
Cu3–I4	2.672(8)	Cu3–S3	2.277(1)
Cu4–I1	2.714(8)	Cu4–I3	2.725(1)
Cu4–I4	2.657(8)	Cu4–S2B	2.303(2)
I1–Cu1–I2	109.06(3)	I1–Cu1–I4	111.46(3)
I2–Cu1–I4	116.79(3)	I1–Cu2–I2	108.99(3)
I1–Cu2–I3	114.36(3)	I2–Cu2–I3	114.37(3)
I2–Cu3–I3	111.96(3)	I2–Cu3–I4	113.85(3)
I3–Cu3–I4	113.94(3)	I1–Cu4–I3	112.03(3)
I1–Cu4–I4	111.98(3)	I3–Cu4–I4	111.82(3)
I1–Cu1–S1	105.86(4)	I2–Cu1–S1	105.90(4)
I4–Cu1–S1	107.04(4)	I3–Cu3–S3	112.07(4)
I4–Cu3–S3	108.73(4)	I2–Cu3–S3	94.71(4)
I1–Cu2–S4B	106.74(4)	I2–Cu2–S4B	109.70(4)
I3–Cu2–S4B	102.16(4)	I1–Cu4–S2B	97.43(4)
I3–Cu4–S2B	102.74(4)	I4–Cu4–S2B	119.85(4)

[a] Symmetry codes: (A) $-x + 1, y + 1/2, -z + 3/2$; (B) $-x, y + 1/2, -z + 3/2$.

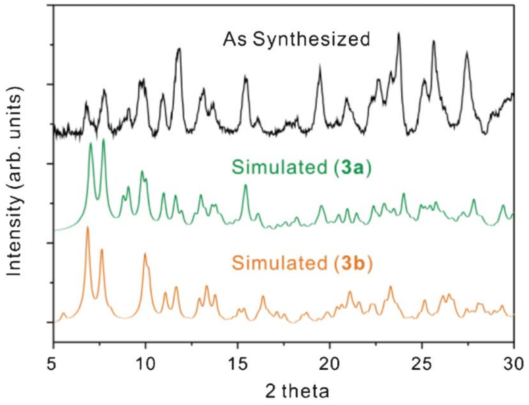

Fig. 5 Comparison of XRPD patterns: (top) as synthesized and (middle) **3a** and (bottom) **3b** simulated from the single crystal X-ray data.

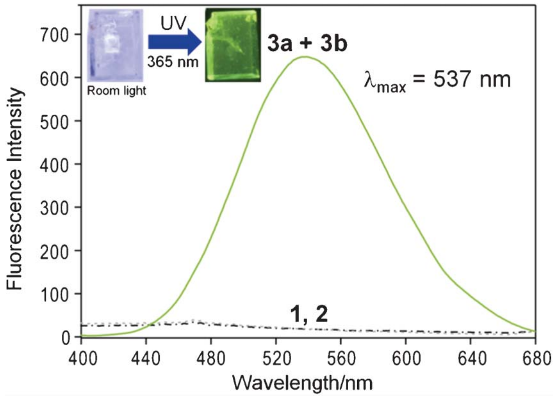

Fig. 6 Solid-state photoluminescence spectra of **1**, **2** and **3a** (with small amount of **3b**) at room temperature (excitation at 343 nm).

carried out on a LECO CHNS-932 elemental analyzer after they were dried in a vacuum at room temperature.

Synthetic details for L

Cs_2CO_3 (8.75 g, 26.9 mmol) was dissolved in DMF (500 mL) in a flask and a syringe was filled with 1,3-bis(2-(chloromethyl)phenoxy)propane (4.16 g, 12.8 mmol) and 1,4-phenylenedimethanethiol (2.17 g, 12.8 mmol) dissolved in DMF (30 mL). Under a nitrogen atmosphere, the contents of the syringe was added at a regular speed (0.6 mL h^{-1}) into the DMF solution maintaining 45–50 °C. After cooling to room temperature the reaction mixture was filtered and the solvent was removed. Water (100 mL) was added and the mixture was extracted with dichloromethane. Flash column chromatography on silica gel using dichloromethane–n-hexane (v/v 3 : 7) gave **L** as a colourless solid. Yield: 65%; Mp: 158–159 °C. ^{1}H NMR (300 MHz, $CDCl_3$): δ 6.78–7.44 (*m*, 12H, Ar), 3.91 (*t*, 4H), 3.73 (*s*, 4H), 3.65 (*s*, 4H), 1.96 (*m*, 2H). ^{13}C NMR (75 MHz, $CDCl_3$): δ 156.51, 137.37, 130.82, 128.54, 126.52, 121.07, 112.4, 65.05, 35.49, 29.54. IR (KBr disk): 2905, 2872, 1582, 1491, 1473, 1450, 1428, 1389, 1290, 1245, 1236, 1185, 1160, 1142, 1126, 1090, 1055, 1020, 953, 826, 749, 708, 686, 560, 456 cm^{-1}. Anal. Calcd for $[C_{25}H_{26}O_2S_2]$: C, 71.05; H, 6.20; S, 15.18. Found: C, 71.31; H, 6.27; S, 15.16%. Mass spectrum: $m/z = 423.08$ $[C_{25}H_{27}O_2S_2]^+$.

Preparation of $[CuCl_2(L)(CH_3CN)]_n$ (1)

Copper(I) chloride (11.7 mg, 0.118 mmol) in acetonitrile was added to a solution of **L** (20.0 mg, 0.047 mmol) in dichloromethane. The initial colourless reaction mixture changed to green within 30 min at room temperature. Slow evaporation of the green solution afforded a brown crystalline product **1** suitable for X-ray analysis. Yield: 20%. Mp: 172–173 °C (decomp.). IR (KBr disk): 2923, 2858, 2362, 1646, 1598, 1491, 1457, 1413, 1286, 1250, 1101, 1040, 1017, 852, 751, 460 cm^{-1}. Anal. Calcd for $[C_{27}H_{29}Cl_2CuNO_2S_2]$: C, 54.22; H, 4.89; N, 2.34; S, 10.72. Found: C, 54.43; H, 4.81; N, 2.36; S, 10.63%.

Table 5 Crystal and experimental data for **L**, **1**, **2**, **3a** and **3b**

	L	**1**	**2**	**3a**	**3b**
Formula	$C_{25}H_{26}O_2S_2$	$C_{27}H_{26}Cl_2CuNO_2S_2$	$C_{54}H_{60}Br_2Cl_8Cu_2O_4S_4$	$C_{51}H_{54}Cl_2Cu_4I_4O_4S_4$	$C_{51}H_{54}Cl_2Cu_4I_4O_4S_4$
T/K	173(2)	173(2)	173(2)	173(2)	173(2)
Formula weight	422.58	595.05	1471.76	1691.84	1691.84
Crystal system	Orthorhombic	Monoclinic	Triclinic	Monoclinic	Monoclinic
Space group	$P2_12_12_1$	$P2_1/c$	$P\bar{1}$	$C2/c$	$P2_1/c$
a/Å	5.5135(2)	11.6776(6)	11.2153(3)	36.215(4)	17.0726(15)
b/Å	8.1356(3)	18.6014(10)	11.6948(3)	13.9659(14)	21.8272(18)
c/Å	47.2858(14)	13.2518(7)	12.9855(4)	28.036(5)	16.3027(14)
α (°)	90	90	85.0890(10)	90	90
β (°)	90	108.458(3)	65.1570(10)	125.048(4)	110.571(4)°
γ (°)	90	90	79.3950(10)	90	90
V/Å^3	2121.03(13)	2730.5(2)	1519.11(7)	11 609(3)	5687.8(8)
Z	4	4	2	8	4
D_c/g cm^{-3}	1.323	1.448	1.609	1.936	1.976
μ/mm^{-1}	0.270	1.174	2.548	3.850	3.929
$2\theta_{max}$ (°)	56.50	56.00	52.00	54.00	56.00
Reflections collected	38 369	49 050	24 176	51 195	53 038
Independent reflections	5243 [R(int) = 0.0356]	6597 [R(int) = 0.1350]	5962 [R(int) = 0.0413]	12 638 [R(int) = 0.0587]	13 702 [R(int) = 0.1450]
Goodness-of-fit on F^2	1.155	1.055	1.062	1.073	1.025
R_1, wR_2 [$I > 2\sigma(I)$]	0.0477, 0.1149	0.0395, 0.1137	0.0321, 0.0864	0.0363, 0.0956	0.0496, 0.1272
R_1, wR_2 (all data)	0.0490, 0.1157	0.0368, 0.0918	0.0348, 0.0885	0.0414, 0.0992	0.0675, 0.1403

Preparation of $\{[(Cu_2Br_2)(L)_2]\cdot 4CH_2Cl_2\}_n$ (2)

Slow diffusion of a dichloromethane solution of **L** (20.0 mg, 0.047 mmol) into an acetonitrile solution of copper(I) bromide (17.0 mg, 0.118 mmol) at room temperature afforded a pale yellow crystalline complex **2**. Yield: 60%. Mp: 199–200 °C (decomp.). IR (KBr disk): 2917, 2871, 1596, 1584, 1511, 1491, 1468, 1453, 1428, 1416, 1400, 1386, 1287, 1239, 1192, 1164, 1152, 1104, 1049, 1029, 951, 901, 757, 705, 673, 499 cm^{-1}. Anal. Calcd for [$C_{52}H_{56}Br_2Cl_4Cu_2O_4S_4$]: C, 47.97; H, 4.34; S, 9.85. Found: C, 48.45; H, 3.82; S, 10.44%.

Preparation of $\{[Cu_4I_4(L)_2]\cdot CH_2Cl_2\}_n$ (3a and 3b as an isomeric mixture)

Slow diffusion of a dichloromethane solution of **L** (20.0 mg, 0.047 mmol) into an acetonitrile solution of copper(I) iodide (22.5 mg, 0.118 mmol) yielded a pale yellow crystalline product. Single crystal X-ray analysis and XRPD results confirmed that the product is a two isomeric mixture of **3a** and **3b** with an identical chemical composition. Separation of the mixed isomeric product was not possible. Yield: 90%. Mp: 194–196 °C (decomp.). IR (KBr disk): 2918, 2871, 1597, 1585, 1508, 1491, 1468, 1453, 1417, 1318, 1289, 1241, 1191, 1163, 1100, 1049, 1028, 955, 889, 853, 834, 751, 697, 565 cm^{-1}. Anal. Calcd for [$C_{51}H_{54}Cu_4Cl_2I_4O_4S_4$]: C, 36.20; H, 3.22; S, 7.58. Found: C, 36.19; H, 3.04; S, 7.51%.

X-ray crystallographic analysis

All data were collected on a Bruker SMART APEX II ULTRA diffractometer equipped with graphite monochromated Mo-Kα radiation (λ = 0.71073 Å) generated by a rotating anode. Data collection, data reduction and semi-empirical absorption correction were carried out using the software package of APEX2.[16] All of the calculations for the structure determination were carried out using the SHELXTL package.[17] In all cases, all non-hydrogen atoms were refined anisotropically and all hydrogen atoms were placed in idealized positions and refined isotropically in a riding manner along with the their respective parent atoms. Relevant crystal data collection and refinement data for the crystal structures of **L**, **1**, **2**, **3a** and **3b** are summarized in Table 5. In the refinement procedure for **L**, the O1–CH_2–CH_2–CH_2–O2 segment is disordered over two sites occupied in a 55 : 45 ratio (Fig. S9†).

Acknowledgements

This work was supported by World Class University (WCU) project (R32-20003) and KRF (2011-0011064), Republic of Korea.

References

1 (*a*) L. F. Lindoy, *Coord. Chem. Rev.*, 1998, **174**, 327; (*b*) R. E. Wolf Jr., J. R. Hartman, J. M. E. Storey, B. M. Foxman and S. R. Cooper, *J. Am. Chem. Soc.*, 1987, **109**, 4328.
2 (*a*) S. Park, S. Y. Lee and S. S. Lee, *Inorg. Chem.*, 2010, **49**, 1238; (*b*) J. Y. Lee, H. J. Kim, J. H. Jung, W. Sim and S. S. Lee, *J. Am. Chem. Soc.*, 2008, **130**, 13838; (*c*) J. Y. Lee, S. Y. Lee, W. Sim, K.-M. Park, J. Kim and S. S. Lee, *J. Am. Chem. Soc.*, 2008, **130**, 6902; (*d*) S. Y. Lee, S. Park, H. J. Kim, J. H. Jung and S. S. Lee, *Inorg. Chem.*, 2008, **47**, 1913; (*e*) J. Y. Lee, S. Y. Lee, J. Seo, C. S. Park, J. N. Go, W. Sim and S. S. Lee, *Inorg. Chem.*, 2007, **46**, 6221; (*f*) I. Yoon, J. Seo, J.-E. Lee, K.-M. Park, M. S. Lah and S. S. Lee, *Inorg. Chem.*, 2006, **45**, 3487; (*g*) J. Seo, M. R. Song, J.-E. Lee, S. Y. Lee, I. Yoon, K.-M. Park, J. Kim, J. H. Jung, S. B. Park and S. S. Lee, *Inorg. Chem.*, 2006, **45**, 952.
3 (*a*) G. H. Robinson and S. A. Sangokova, *J. Am. Chem. Soc.*, 1988, **110**, 1494; (*b*) J. Buter, R. M. Kellog and F. van Bolhuis, *J. Chem. Soc., Chem. Commun.*, 1991, 910; (*c*) A. J. Blake, R. O. Gould, S. Parsons, C. Radek and M. Schröder, *Angew. Chem., Int. Ed. Engl.*, 1995, **34**, 2374; (*d*) M. Heller and W. S. Sheldrick, *Z. Anorg. Allg. Chem.*, 2004, **630**, 1191; (*e*) B. de Groot, H. A. Jenkins and S. J. Loeb, *Inorg. Chem.*, 1992, **31**, 203; (*f*) G. J. Grant, D. F. Galas, M. W. Jones, K. D. Loveday, W. T. Pennington, G. L. Schimek, C. T. Eagle and D. G. VanDerveer, *Inorg. Chem.*, 1998, **37**, 5299.
4 H. J. Kim and S. S. Lee, *Inorg. Chem.*, 2008, **47**, 10807.
5 S. J. Lee, J. H. Jung, J. Seo, I. Yoon, K.-M. Park, L. F. Lindoy and S. S. Lee, *Org. Lett.*, 2006, **8**, 1641.
6 H. J. Kim, L. F. Lindoy and S. S. Lee, *Cryst. Growth Des.*, 2010, **10**, 3850.
7 (*a*) P. C. Ford, E. Cariati and J. Bourassa, *Chem. Rev.*, 1999, **99**, 3625; (*b*) T. H. Kim, Y. W. Shin, J. H. Jung, J. S. Kim and J. Kim,

Angew. Chem., Int. Ed., 2008, **47**, 685; (*c*) P. D. Harvey and M. Knorr, *Macromol. Rapid Commun.*, 2010, **31**, 808.

8 R. Peng, M. Li and D. Li, *Coord. Chem. Rev.*, 2010, **254**, 1.

9 M. Jo, J. Seo, L. F. Lindoy and S. S. Lee, *Dalton Trans.*, 2009, 6096.

10 (*a*) S. Park, S. Y. Lee, M. Jo, J. Y. Lee and S. S. Lee, *CrystEngComm*, 2009, **11**, 43; (*b*) S. Lee, S. Park, Y. Kang, S.-H. Moon, S. S. Lee and K.-M. Park, *Bull. Korean Chem. Soc.*, 2008, **29**, 1811.

11 Y. A. Ibrahim, A. H. M. Elwahy and G. M. M. Elkareish, *J. Chem. Res. (S)*, 1994, **11**, 414.

12 (*a*) H. J. Kim, Y. Jin, J. Seo, J.-E. Lee, J. Y. Lee and S. S. Lee, *Inorg. Chem. Commun.*, 2006, **9**, 1040; (*b*) K.-M. Park, I. Yoon, J. Seo, J.-E. Lee, J. Kim, K. S. Choi, O.-S. Jung and S. S. Lee, *Cryst. Growth Des.*, 2005, **5**, 1707; (*c*) M. Heller and W. S. Sheldrick, *Z. Anorg. Allg. Chem.*, 2003, **629**, 1589; (*d*) N. R. Brooks, A. J. Brake, N. R. Champness, P. A. Cooke, P. Hubberstey, D. M. Proserpio, C. Wilson and M. Schröder, *J. Chem. Soc., Dalton Trans.*, 2001, 456; (*e*) R. D. Adams, M. Huang and S. Johnson, *Polyhedron*, 1998, **17**, 2775; (*f*) M. Munakata, L. P. Wu, T. Kuroda-Sowa, M. Maekawa, Y. Suenaga and S. Nakagawa, *J. Chem. Soc., Dalton Trans.*, 1996, 1525; (*g*) L. Chen, L. K. Thompson and J. N. Bridson, *Can. J. Chem.*, 1992, **70**, 2709.

13 (*a*) S. Y. Lee, S. Park and S. S. Lee, *Inorg. Chem.*, 2009, **48**, 11335; (*b*) H. J. Kim, M. R. Song, S. Y. Lee, J. Y. Lee and S. S. Lee, *Eur. J. Inorg. Chem.*, 2008, 3532.

14 (*a*) M. R. Churchill and F. J. Rotella, *Inorg. Chem.*, 1977, **16**, 3267; (*b*) O. A. Babich and V. N. Kokozay, *Polyhedron*, 1997, **16**, 1487; (*c*) P. R. Ashton, A. L. Burns, C. G. Claessens, G. K. H. Shimizu, K. Small, J. F. Stoddart, A. J. P. White and D. J. Williams, *J. Chem. Soc., Dalton Trans.*, 1997, 1493; (*d*) P. M. Graham and R. D. Pike, *Inorg. Chem.*, 2000, **39**, 5121; (*e*) M. Vitale, W. E. Palke and P. C. Ford, *J. Phys. Chem.*, 1992, **96**, 8329; (*f*) T. H. Kim, K. Y. Lee, Y. W. Shin, S.-T. Moon, K.-M. Park, J. S. Kim, Y. Kang, S. S. Lee and J. Kim, *Inorg. Chem. Commun.*, 2005, **8**, 27.

15 (*a*) I.-H. Park and S. S. Lee, *CrystEngComm*, 2011, **13**, 6520; (*b*) Y. Jin, H. J. Kim, J. Y. Lee, S. Y. Lee, W. J. Shim, S. H. Hong and S. S. Lee, *Inorg. Chem.*, 2010, **49**, 10241.

16 Bruker, *APEX2 Version 2009.1-0 Data collection and Processing Software*, Bruker AXS Inc., Madison, Wisconsin, USA, 2008.

17 Bruker, *SHELXTL-PC Version 6.22 Program for Solution and Refinement of Crystal Structures*, Bruker AXS Inc., Madison, Wisconsin, USA, 2001.